

Synthesis and molecular properties of nerve agent reactivator HLö-7 dimethanesulfonate

Fu-Lian Hsu¹, Su Y. Bae¹, Jack McGuire², Dana R Anderson³, Stephanie M. Bester², Jude J. Height¹, Scott D. Pegan^{*1,2,3} and Andrew J. Walz^{*1}

¹*United States Army Edgewood Chemical Biological Center, Aberdeen Proving Ground, Maryland, United States of America*

²*Department of Pharmaceutical and Biomedical Sciences, University of Georgia, Athens, Georgia, United States of America,*

³*United States Research Institute of Chemical Defense, Aberdeen Proving Ground, Maryland, United States of America*

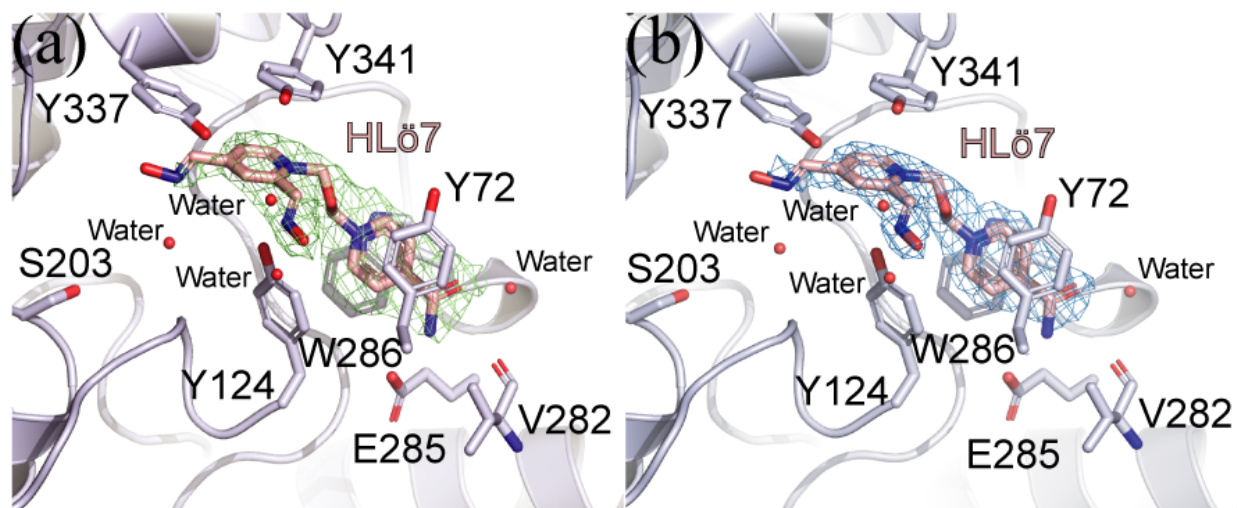
Contents:

Supplemental Table 1. Data collection and refinement statistics.	2
Supplemental Figure 1. Electron density of HLö-7 within the hAChE active site	3
Supplemental Figure 2. X-ray crystal structure of HLö-7 bound to hAChE and mAChE inhibited by tabun	3
Supplemental Figure 3. HLö-7 reactivation of muscle force inhibited by VX, GF or GB.	4
Supplemental Figure 4. HLö-7, HI-6, MMB-4 and 2-PAM (200 uM dose) reactivation of muscle force inhibited by GF or GB	4
Supplemental Figure 5. Experimental protocol for the MPNH studies.	5
Supplemental Figure 6. Representative tetanic contractions for the four experimental phases.	5
Supplemental Figure 7. ¹ H NMR spectrum of HLö-7 DMS in D ₂ O.	6
Supplemental Figure 8. ¹³ C NMR spectrum of HLö-7 DMS in D ₂ O.	7
X-Ray Crystallography Experimental.	7
Mouse Phrenic Nerve Hemidiaphragm Assay Experimental	8
References	8

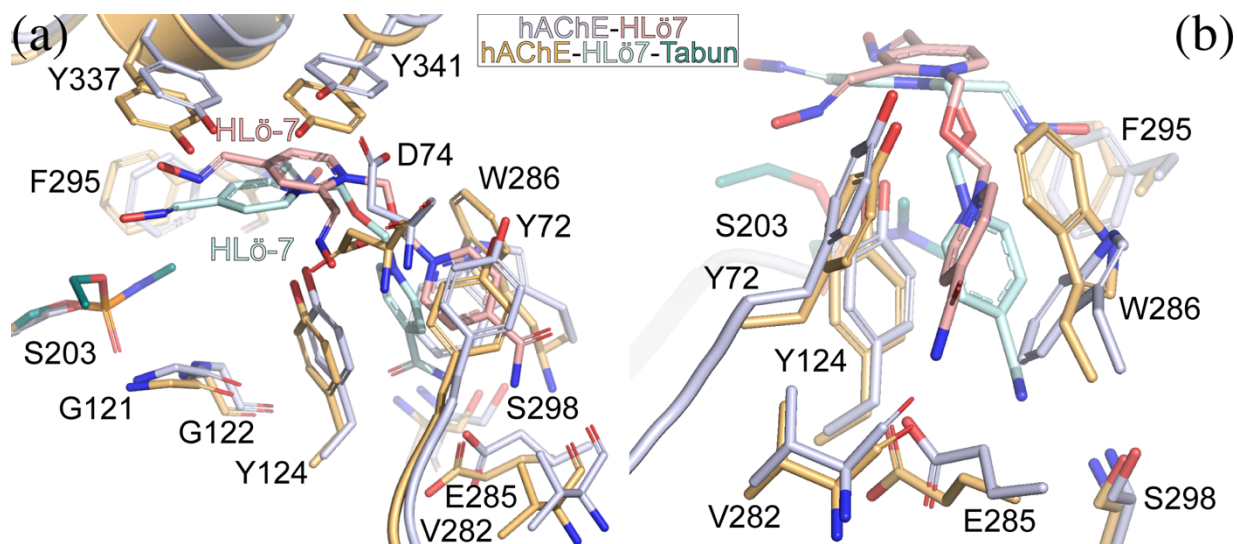
Supplemental Table 1. Data collection and refinement statistics

AChE-HL67	
Data collection	
Space group	P 3 1 2 1
Cell dimensions	
<i>a</i> , <i>b</i> , <i>c</i> (Å)	104.7, 104.7, 324.2
α , β , γ (°)	90.0, 90.0, 120.0
Resolution (Å)	50.0 – 2.42 (2.46-2.42)
Completeness (%)	99.5 (99.3)
<i>R</i> _{merge} (%)	11.1 (62.9)
<i>R</i> _{pim} (%)	5.3 (33.5)
CC 1/2	(0.816)
<i>I</i> / σ <i>I</i>	12.9 (2.5)
Redundancy	5.6 (4.4)
Refinement	
Resolution (Å)	41.25-2.42 (2.51-2.42)
No. reflections	79580
<i>R</i> _{work} / <i>R</i> _{free} (%)	16.08/19.15
No. atoms	
Protein	8289
Ligand/ion	190
Water	699
B-factors	
Protein	49.2
Ligand/ion	105.2
Water	60.4
R.m.s deviations	
Bond lengths (Å)	0.006
Bond angles (°)	0.86

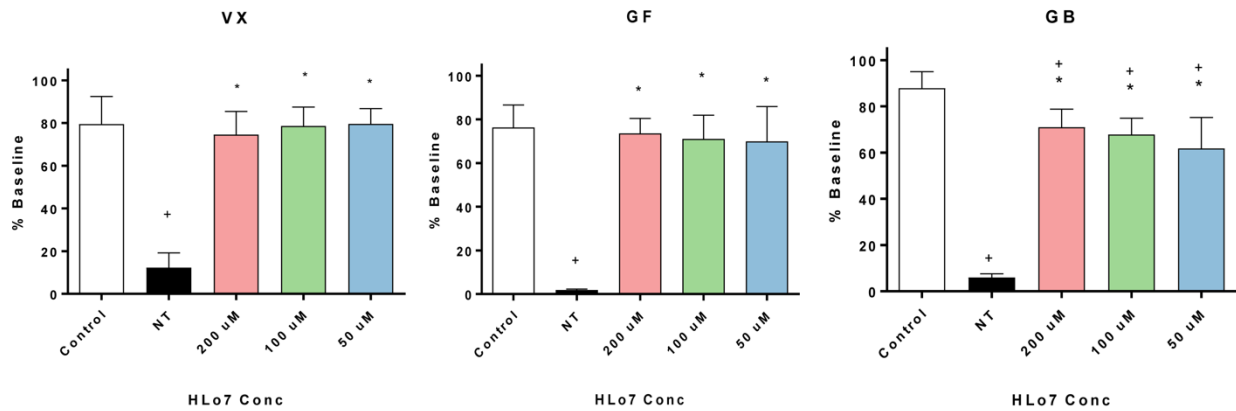
Supplemental Figure 1. Electron density of HLö-7 within the hAChE active site. (a) Close-up of HLö-7 (pink) interacting with hAChE (light blue) and waters (red spheres). Green mesh represents $F_o - F_c$ density scaled to 3σ (b) Coloring for hAChE and HLö-7 are the same as in (a) with blue mesh representing $2F_o - F_c$ density scaled to 3σ .



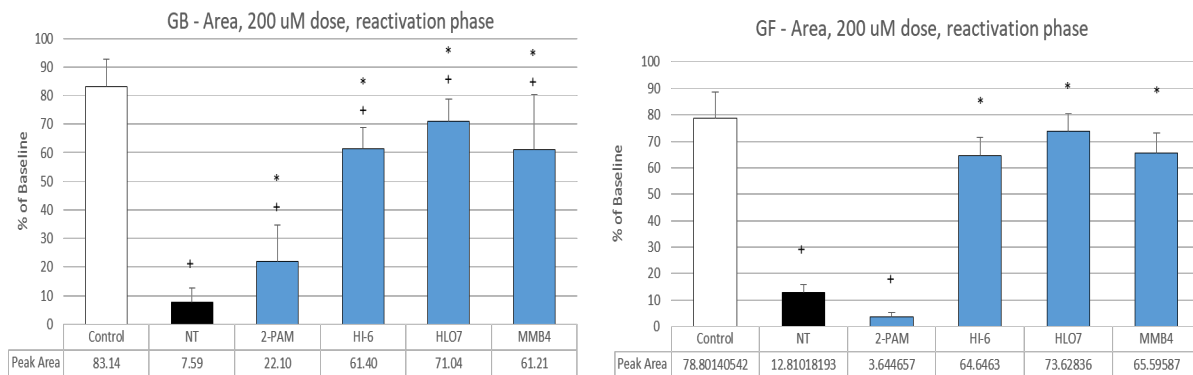
Supplemental Figure 2. X-ray crystal structure of HLö-7 bound to hAChE and mAChE inhibited by tabun. (a-b) The active site of hAChE-HLö-7 (light blue-pink) overlaid with the active site of mAChE (gold) inhibited by tabun (dark teal) and bound to HLö 7 (light cyan). Waters are shown as red balls. Hydrogen bonds represented by black dashed lines. Measurements are in angstroms and labeled in red.



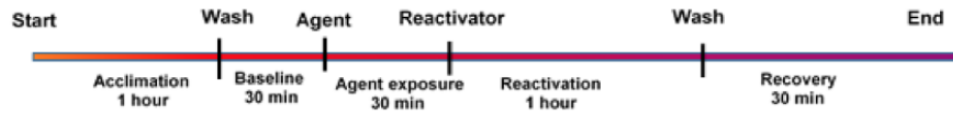
Supplemental Figure 3. HL δ -7 reactivation of muscle force inhibited by VX, GF or GB. Data shown are the mean area under the tetanic contraction curve during the reactivation phase (N=6-8 per datapoint). * = different from no treatment (NT); + = different from Control.



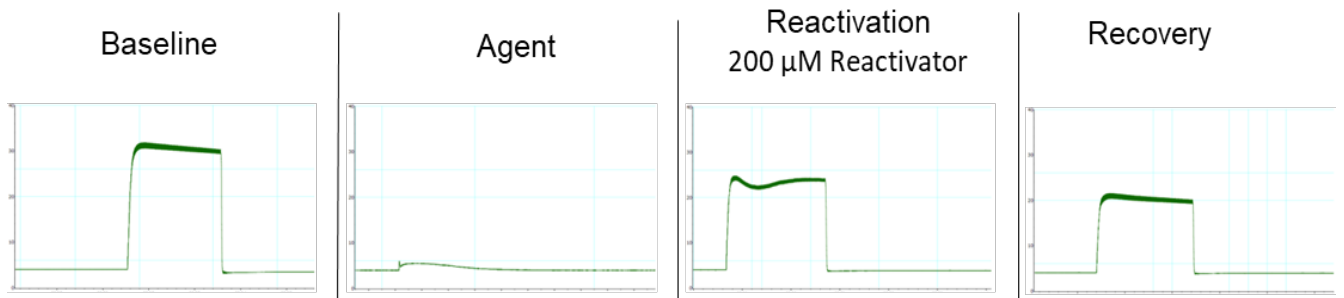
Supplemental Figure 4. HL δ -7, HI-6, MMB-4 and 2-PAM (200 μ M dose) reactivation of muscle force inhibited by GF or GB. Data shown are the mean area under the tetanic contraction curve during the reactivation phase (N=6-8 per datapoint). * = different from no treatment (NT); + = different from Control.



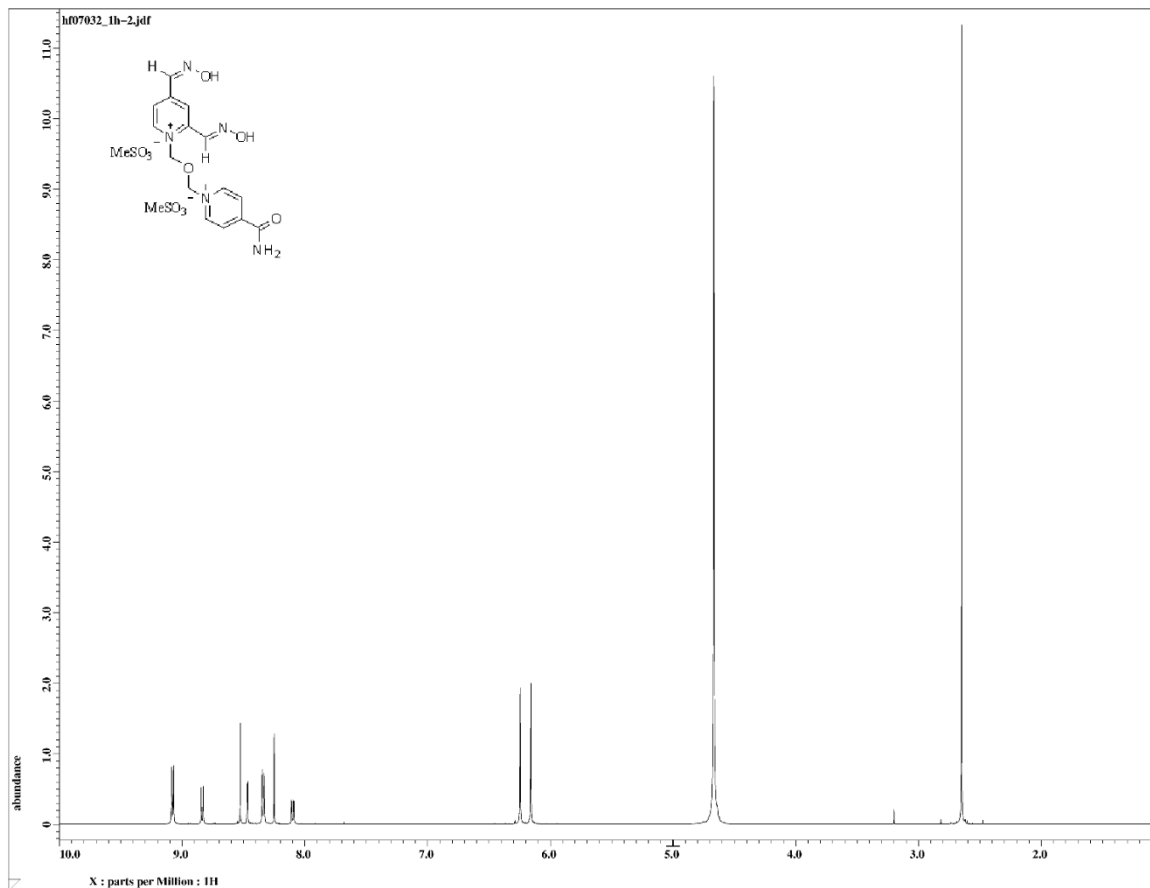
Supplemental Figure 5. Experimental protocol for the MPNH studies¹.



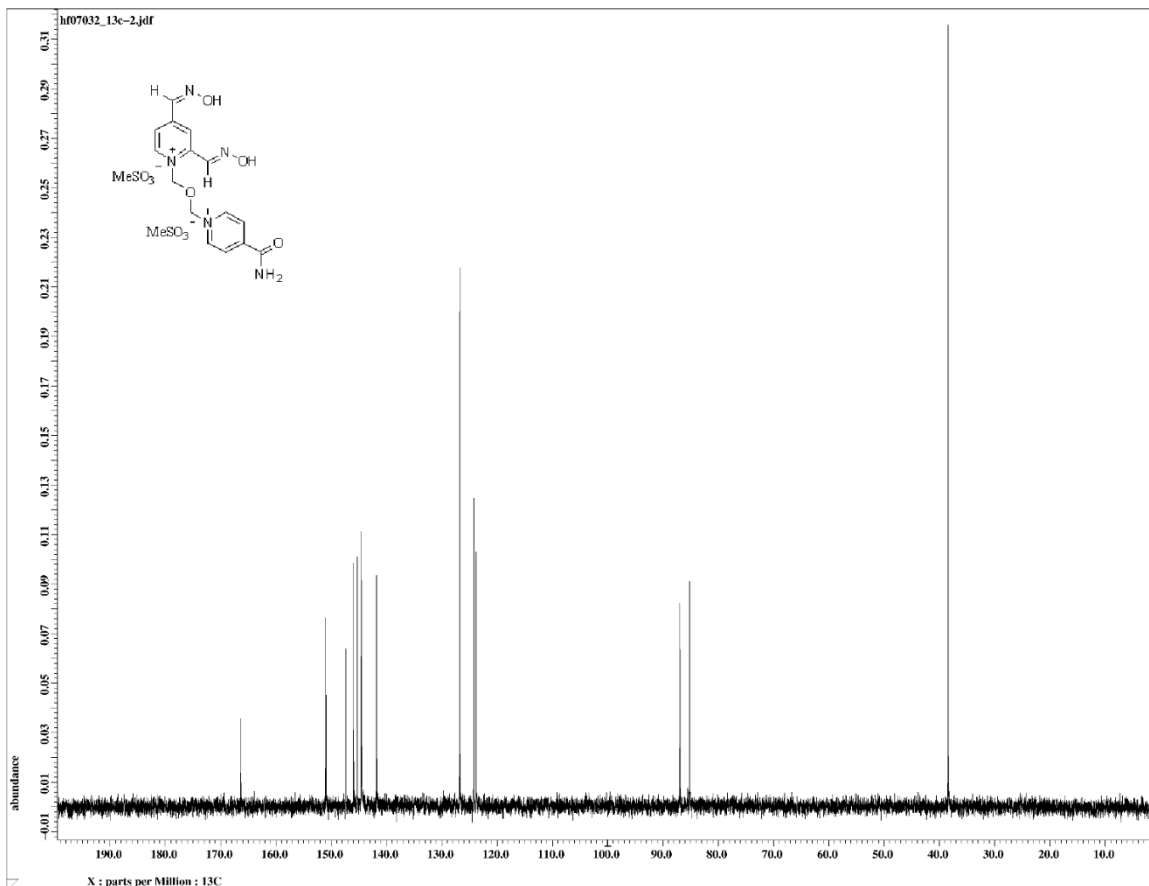
Supplemental Figure 6. Representative tetanic contractions for the four MPNH experimental phases.



Supplemental Figure 7. ^1H NMR spectrum of HLö-7 DMS in D_2O .



Supplemental Figure 8. ^{13}C NMR spectrum of HLö-7 DMS in D_2O .



X-ray Crystallography Experimental

Cloning, expression, and purification of a 1-574 amino acid construct of hAChE for crystallization is as previously described^{2,3}. The protein was dialyzed overnight into 10 mM HEPES pH 7.0, and 10 mM NaCl and concentrated to 16 mg/mL. Using previously reported procedures^{2,3} hAChE was crystallized in 15-21% polyethylene glycol 3350 (PEG) and 0.17-0.21 M potassium nitrate. The hexagonal rod-shaped crystals were soaked in a cryogenic solution of 25% polyethylene glycol 3350 (PEG) and 0.17-0.21 M potassium nitrate supplemented with 1 mM HLö-7 DMS for 12 minutes prior to being mounted on polymer loops and flash frozen in liquid nitrogen. Data sets were collected for the hAChE-HLö-7 structure at 22-ID beamline of SERCAT. The HKL2000 suite was used to process and scale data sets⁴. Cross-validation drawn from a random 5% of the reflections was performed using the CCP4 software suite⁵. Molecular replacement was used to obtain initial phases using Phaser with 4EY4² as a search model⁶. The structure was further refined manually using Coot⁷ and Phenix.Refine⁸. Molprobit⁹ was used to confirm the quality of the

structure. X-ray crystallographic statistics regarding the data and the final structure are in Table S1. The structure was deposited as PDB entry 6NEA.

Mouse Phrenic Nerve Hemidiaphragm Assay Experimental

Male C57/Bl6 mice 8-10 weeks old were used for all studies. The *ex vivo* phrenic nerve hemidiaphragm preps were run in a Radnoti tissue bath system: Hemidiaphragm/phrenic nerve bundles/ribs were dissected and maintained in tissue baths with oxygenated (95%O₂/5%CO₂) Tyrode's buffer solution at 37°C. Tetanic stimulation parameters were 100 Hz, 2 sec train, 5 volts, resting tension ~3.5 g every 10 min. The agent bath concentration used was 5 x 10⁻⁶ M for GB and 1 x 10⁻⁷ M for both GF and VX. The bath concentrations for HLö-7 were 200 µM, 100 µM and 50 µM. Additional data is shown (Figure S4) for studies using the 200 µM doses of the oximes HI-6, MMB-4 and 2-PAM. Hemidiaphragm preps were placed in individual tissue baths and acclimated for 1 hour with tetanic stimulation applied every 10 min throughout acclimation and each of the four experimental phases (baseline, agent, reactivation, recovery). The experimental protocol and representative model can be found in Figure S4 and S5. Tyrode's buffer is then drained, and fresh buffer added. Baseline data is collected for 30 min. Buffer is drained and replaced. Agent is immediately added, and 30 min of agent exposure data is collected. Agent/Buffer is drained and replaced with reactivator in buffer. One hour of data is collected for the reactivation phase. Buffer is drained and replaced with fresh buffer. Thirty min of data is collected for the recovery phase. At the end of the experimental protocol the diaphragm is collected, weighed and homogenized in 1% Triton X-100 1:9 for AChE activity determination. As indicated by previous studies¹⁰, the Triton X-100 used to homogenize the tissue in this assay inhibits butyrylcholinesterase leaving only AChE activity being measured. AChE activity was determined utilizing a modified Ellman colorimetric assay^{11,12}. A BCA protein assay was used to normalize enzymatic activity levels to total protein content, giving final values in µmol substrate hydrolyzed/min/g protein.

References.

1. Millard, C. B. K., G.; Ordentlich, A.; Greenblatt, H. M.; Harel, M.; Raves, M. L.; Segall, Y.; Barak, D.; Shafferman, A.; Silman, I.; Sussman, J. L. Crystal Structures of Aged Phosphonylated Acetylcholinesterase: Nerve Agent Reaction Products at the Atomic Level. *Biochemistry* **1999**, *38* (22), 7032-7039.
2. Cheung, J. R., M. J.; Burshteyn, F.; Cassidy, M. S.; Gary, E. N.; Love, J.; Franklin, M. C.; Height, J. J. Structures of human acetylcholinesterase in complex with pharmacologically important ligands. *J Med Chem* **2012**, *55*, 10282-10286.
3. Franklin, M. C. R., M. J.; Ginter, C.; Cassidy, M. S.; Cheung, J. Structures of paraoxon-inhibited human acetylcholinesterase reveal perturbations of the acyl loop and the dimer interface. *Proteins* **2016**, *84* (9), 1246-1256.
4. Otwinowski, Z. M., W. Processing of X-ray Diffraction Data Collected in Oscillation Mode. *Methods in Enzymology* **1997**, *276*, 307-326.
5. Winn, M. D. B., C. C.; Cowtan, K. D.; Dodson, E. J.; Emsley, P.; Evans, P. R.; Keegan, R. M.; Krissinel, E. B.; Leslie, A. G.; McCoy, A.; McNicholas, S. J.; Murshudov, G. N.; Pannu, N. S.; Potterton, E. A.; Powell, H. R.; Read,

- R. J.; Vagin, A.; Wil. Overview of the CCP4 suite and current developments. *Acta Crystallogr D Biol Crystallogr* **2011**, *67 (Pt 4)*, 235-242.
6. McCoy, A. J. G.-K., R. W.; Adams, P. D.; Winn, M. D.; Storoni, L. C.; Read, R. J. Phaser crystallographic software. *J Appl Crystallogr* **2007**, *40 (Pt 4)*, 658-674.
 7. Emsley, P. C., K. Coot: model-building tools for molecular graphics. *Acta Crystallogr D Biol Crystallogr* **2004**, *60 (Pt 12 Pt 1)*, 2126-2132.
 8. Adams, P. D. A., P. V.; Bunkoczi, G.; Chen, V. B.; Davis, I. W.; Echols, N.; Headd, J. J.; Hung, L. W.; Kapral, G. J.; Grosse-Kunstleve, R. W.; McCoy, A. J.; Moriarty, N. W.; Oeffner, R.; Read, R. J.; Richardson, D. C.; Richardson, J. S.; Terwilliger. PHENIX: a comprehensive Python-based system for macromolecular structure solution. *Acta Crystallogr D Biol Crystallogr* **2010**, *66 (Pt 2)*, 213-221.
 9. Chen, V. B. A., W. B. . 3.; Headd, J. J.; Keedy, D. A.; Immormino, R. M.; Kapral, G. J.; Murray, L. W.; Richardson, J. S.; Richardson, D. C. MolProbity: all-atom structure validation for macromolecular crystallography. *Acta Crystallogr D Biol Crystallogr* **2010**, *66*, 12-21.
 10. Thiermann, H. E., P.; Worek, F. Muscle force and acetylcholinesterase activity in mouse hemidiaphragms exposed to paraoxon and treated by oximes in vitro. *Toxicology* **2010**, *272*, 46-51.
 11. Ellman, G. L. C., K. D.; Andres, V. . J.; Feather-Stone, R. M. A new and rapid colorimetric determination of acetylcholinesterase activity. *Biochem Pharmacol* **1961**, *7*, 88-95.
 12. Shih, T. M. S., J. W.; O'Donnell, J. C.; McDonough, J. H. Evaluation of nine oximes on in vivo reactivation of blood, brain, and tissue cholinesterase activity inhibited by organophosphorus nerve agents at lethal dose. *Toxicol Mech Methods* **2009**, *19*, 386-400.